JOURNAL OF MATERIALS SCIENCE 29 (1994) 6011–6018

Experimental verification of quantum structural diagrams: formation by ion-beam mixing of new quasicrystals $Ga_{85}Mn_{15}$ and $Al_{73}Ni_{16}Ta_{11}$

J. TARTAS*, E. J. KNYSTAUTAS
Département de physique, Université Laval, Québec, Canada G1K 7P4

New quasicrystalline phases in $Ga_{85}Mn_{15}$ and $Al_{73}Ni_{16}Ta_{11}$ alloys have been formed by ion-beam mixing under specific irradiation conditions. These alloys are two of several predictions established on a systematic approach developed using the quantum structural diagrams technique. Microstructural analysis on a micrometre scale was performed under a transmission electron microscope using the selected area diffraction technique. Detailed information is presented on the different solid phases formed as a function of the implantation temperature and of the dose. The diffraction patterns obtained were analysed by elimination of all known or probable crystalline structures, and indexed using a standard indexing scheme for quasicrystals. These patterns are very different from those typical of Al-based quasicrystals, both in intensities and in interplanar spacings, although comparable values were found for d_0, the quasicrystalline lattice constant.

1. Introduction

While their exact microstructure is still largely an open question, due to numerous experimental difficulties related to the determination of at least two unit cells, quasicrystals have become well established as a new fundamental form of solid matter, since their recent discovery [1]. Despite much theoretical work on possible structural models, little is known with certainty about the physical, chemical or thermodynamic factors responsible for their formation and growth. Even more problematic is the precise prediction of probable new quasicrystals, i.e. the specification of both elements and concentrations. This is not a trivial unimportant problem, as there are 'stoichiometric' quasicrystals within very restricted concentration ranges. For example, the $Pd_6U_2Si_2$ quasicrystal has been found to exist within a variation of atomic concentrations of only 1% [2], which indicates a strong chemical ordering.

We have addressed this problem by developing an approach based on quantum structural diagrams [3]. Quasicrystals have been separated into subgroups, a concept based on a simple and general classification of alloys, which is in turn based on an ordering of concentrations that takes into account what kinds of major and minor constituent elements exist in the alloy. Such subgroups occupy small areas on these diagrams, which permit one (independently of the experimental technique used) to predict likely candidates for quasicrystalline formation. Surprisingly, our predictions show that there is a significant number of quasicrystals that contain Ga, In and Tl as the main component, although no quasicrystals have been discovered for such cases (see below). These predictions are consistent with the fact that these main elements belong to the same chemical group, and with the observation that the density of valence electronic states of these elements is well described by the nearly free electron model, as is the case for Al [4]. This fact alone does not guarantee these predictions; other predictions we have made are very different in nature. Our finding is very different from other predictions established via different (and somewhat arbitrary) approaches which are also based on quantum structural diagrams [5]. In order to test our main conclusion, we have checked by ion beam mixing two of these predictions: $Ga_{85}Mn_{15}$ and $Al_{73}Ni_{16}Ta_{11}$. In this paper, the formation of these quasicrystals is described, to the best of our knowledge, for the first time.

The first prediction ($Ga_{85}Mn_{15}$) has been chosen because, unlike In and Tl which have never been found in any quasicrystalline alloy, Ga is a minor component of the ternary quasicrystal $Zn_5Mg_3Ga_2$ [6], although no binary quasicrystal is known to contain it. Also, as the quasicrystal $Al_{85}Mn_{15}$ has been obtained by a large variety of experimental techniques [7], we would also expect favourable kinetic factors in this case, given the chemical similarity between Al and Ga. We have been more prudent concerning the ternary prediction ($Al_{73}Ni_{16}Ta_{11}$) as it is based on Al, as are most quasicrystals. Nevertheless, there is a challenge in this prediction as an attempt by another technique [8] to form the quasicrystal $Al_{85}Ta_{15}$ has been made without success. This ternary prediction is not included in our final list in [3], but is clearly located within the *ddp* subgroup in Figure 1 of [3], and

Present address CÉGEP Edouard-Montpetit, Longueuil (Quebec) Canada J4H 3M6

0022–2461

provides another severe test of our model. On the other hand, several Al-based ternary quasicrystals containing Ni or Ta have been found.

2. Experimental procedure

Multilayered samples were produced by electron-gun evaporation of high-purity elements (at least 99.99%) at room temperature (RT), at a typical base pressure of 1.5×10^{-5} Torr and a typical evaporation rate of a few nm s^{-1}, controlled by a Temescal piezoelectric thickness monitor. During the evaporation process, the pressure measured was typically doubled. $Ga_{85}Mn_{15}$ and $Al_{73}Ni_{16}Ta_{11}$ samples consisted respectively of four sets of two (Ga:21.8/Mn:2.5 nm) and three (Al:17.2/Ni:2.5/Ta:2.8 nm) alternating elemental layers on glass plates previously coated with NaCl. Total thicknesses were then 97.3 and 90.0 nm, respectively, and were based on calibrations made against a Sloan Dektak II mechanical thickness measuring device. Individual layer thicknesses were calculated as a function of relative concentrations by using atomic masses and known densities of the corresponding elemental crystals.

Because of the particular geometry used, limited by the available space in the vacuum system and by the relatively large samples, a maximum variation of atomic concentrations was estimated, of the order of 15% with respect to the mean values (in the chemical formula), which were taken at the centre of the glass plates. Smaller samples were made for ion-beam mixing by detaching the multilayered film from the plate in triply-distilled water and fixing it onto several fine Ni or Cu 200-mesh grids, that also served as a physical support for transmission electron microscope (TEM) examination. Thus some of these small samples were expected to present non-negligible deviations in relative atomic concentrations from the mean values, which might affect the verification of the predictions. This is why most significant results were repeated at least once to ensure their reproducibility. For instance, the ion-beam mixing results in Table II (below) concerning $Ga_{85}Mn_{15}$ have been checked three times at 130 °C to ascertain the non-existence of a quasicrystalline phase. Similarly, the appearance of a quasicrystal at 180 °C for $Al_{73}Ni_{16}Ta_{11}$ has been verified twice.

Ion-beam mixing by 230 keV Ar^{++} ions was done under a typical base pressure less than 5×10^{-7} Torr and a typical pressure less than 2.5×10^{-6} Torr during irradiation. The implantation energy was such that about 70% of the incident ions passed completely through the film, as determined from a TRIM simulation [9] or from projected range tables [10, 11]. The ion-beam current density was 2–6 μA cm^{-2}, as measured by Faraday cups with secondary electron suppression. The spatial distribution of the ion beam of a typical transverse area of 1.5 cm^2 was visually estimated to be sufficiently uniform. For both predictions, a series of experiments was carried out by varying either the implantation temperature T or the dose D, which covered the following intervals: RT $\leq T(°C) \leq 350$ and $0 \leq D(10^{15}\ Ar^{++}\ cm^{-2}) \leq 70$. These intervals contain all values of T and D for which one can reasonably expect quasicrystal formation, as can be deduced from the literature [12–29]. The case $D = 0$ was considered to determine whether quasicrystal formation could take place by interdiffusion of elemental layers at different temperatures. A temperature increment of about 50 °C was used, as it is well known that solid phases, stable or metastable, ordinarily exist over several hundreds of degrees before a phase transition occurs. Therefore the appearance and disappearance of a quasicrystalline phase within such a small temperature interval would be very unlikely. During irradiation, the temperature was maintained within ± 5 °C with respect to the mean value. Each sample was heated to, and kept at, the irradiation temperature for at least 2 h before mixing began.

Microstructural analysis was performed under a transmission electron microscope (Phillips EM420) at 120 keV using the selected area diffraction (SAD) technique [30] over regions on the specimen of 1, 2 and 5 μm, by using appropriate diaphragms. As samples were treated by ion-beam mixing, most diffraction patterns would be expected to exhibit circles rather than points, because typical microcrystalline grain dimensions are of the order of a few tens of nm [31], much smaller than the regions spanned by the electron beam. As for most microstructural studies of quasicrystals using electron diffraction, we aimed simply to identify quasicrystalline phases, by concentrating on interplanar spacings, and fitting them to an indexing scheme while neglecting line intensities. In contrast to crystals, where there is a single unit cell, one cannot separate the structure factor into two independent contributions [32], one pertaining to the type of lattice (or isomorphism class for Penrose tilings), and the other to the repeating motif or base. There are an infinite number of possible Penrose tilings for a given isomorphism class, a problem that is amplified by more or less arbitrary decisions that must be taken in decorating the tiling with atoms to give a realistic microstructure [33]. There are also other difficult problems associated with other structural models such as the icosahedral glass [34] where the introduction of a considerable amount of disorder only permits a statistical description. The main practical consequence is that it is impossible to deduce the exact microstructure from diffraction data only. Nevertheless, it is reasonable to believe that a successful indexing based on a quasicrystalline scheme alone (that is, excluding all known or probable stable or metastable crystalline phases) lends strong support to a quasicrystalline structure, or to a microstructure close to it, i.e. a crystal with a very large unit cell (crystalline approximant). However, this large-cell crystalline structure is considered improbable as it requires long-range cohesion forces to be established (in order to maintain periodicity) within very short times (of the order of 10^{-12} s [35]) by ballistic processes occurring during the relaxation period. Also, the very high cooling rate associated with the ion-beam mixing technique (of the order of 10^{13} K s^{-1}) strongly favours metastable solid phases with a high nucleation rate such as quasicrystals.

Most researchers have used the scheme of Bancel *et al.* [36], which does not seem to provide strong conditions for quasicrystallinity. We instead used the indexation method of Cahn *et al.* [37], where the main advantage is that it gives a well defined, unique succession of strong reflections within the quasicrystalline model. Accordingly, every strong reflection is represented by Q_0 which can be written as a function of two positive integers, N and M_0

$$Q_0^2 = N + \tau M_0 \quad (1)$$

where $M_0 = 4$ INT $(N\tau/4)$, INT(x) refers to the integer part of x, $\tau = (1 + 5^{1/2})/2 = 1.618034\ldots$ is the golden mean, and N is an even integer. For example, for $N = 40$, one finds $M_0 = 64$ and $Q_0^2 = 143.55$. According to [38] (for a single-element quasicrystal with atoms on the vertices of a Penrose lattice), the intensity of the reflection should be roughly correlated to the inverse of the norm of Q' where $Q'^2 = \tau(N\tau - M_0)$. A very weak correlation is found with experimental intensity data for X-rays diffracted by $Al_{86}Mn_{14}$ [37]. By analogy to crystalline structures, the interplanar spacing d is given by [37]

$$d = d_0/(N + \tau M_0)^{1/2} \quad (2)$$

where d_0 is a quasicrystalline parameter closely related to the dimensions of Penrose rhombohedra. Unlike crystals, interplanar spacings in quasicrystals are not constant along a given direction in space. With the well known Bragg law [39], d can be related to experimental conditions. Thus it is possible to systematically classify [37] all observed X-ray reflections by (N, M_0) without any omissions for $Al_{86}Mn_{14}$.

To analyse our electron diffraction data, the first step was to check whether they could be indexed by the quasicrystalline model, then by any probable crystalline phase. To this end, each observed interplanar spacing was divided by the smallest one, thus giving ratios greater than unity that could easily be compared with typical values of crystalline systems in which each reflection can be indexed by three integer indices h, k and l [39]. For instance, for cubic systems, interplanar spacings d are given by: $d^2 = a^2/N^2$ where a is the side length of the conventional cell and $N^2 = (h^2 + k^2 + l^2)$ is a positive integer. We can then express ratios of ds in terms of those of measured radii R on the photographic plate: $R^2/R_{ref}^2 = d_{ref}^2/d^2 = N^2/N_{ref}^2$ with respect to a reference reflection which is normally the smallest diffraction circle. We then obtain

$$N_{ref}^2 R^2/R_{ref}^2 = N^2 = \text{integer} \quad (3)$$

Thus, by multiplying experimental values R^2/R_{ref}^2 by an appropriate integer N_{ref}^2 (which is usually less than about 5), observed reflections can be described by a series of integers N^2, within experimental error. For systems other than cubic, this approach obviously fails. However, we can always limit ourselves to reflections for which one or two indices are equal to zero, and this gives enough such integer reflections to verify with reasonable certainty the possible presence of a crystalline phase, as in general, reflections with the lowest indices are always observed. Such reflections correspond to the highest d values along highly symmetric crystallographic directions which primarily define the actual structure. Once these reflections have been recognized, it is then possible to determine one of the unit cell parameters and restart the procedure to find others, until all parameters have been determined. Table I summarizes all ten first N^2 integer reflections for all crystalline systems.

While missing reflections (when the structure factor is vanishing) for these series are possible, all observed ones will be contained therein. In addition, for non-cubic systems, $N_{ref}^2(R^2/R_{ref}^2)$ can be non-integral, independently of the choice of N_{ref}, which means that the choice of the reference reflection does not correspond to the series we are looking for, i.e. to the corresponding restrictions on indices. Nevertheless, all ratios between the integers in Table I will be kept in this case.

3. Results, analysis and discussion

3.1. Summary of ion-beam mixing experiments

All significant results from the microstructural analysis as a function of the dose D and the implantation temperature T have been summarized in Table II for both alloys studied. Two new quasicrystals appear to have been formed for well-defined dose and temperature ranges. It should be mentioned that no quasicrystalline point diffraction pattern was seen. Surface textures of both specimens showed little variation with D or T. No particular feature typical of rapidly quenched alloys, such as dentritic formation and solidification morphologies, was seen on a micrometre scale for both alloys, although some small, nearly spherical precipitates have been observed for $Ga_{85}Mn_{15}$.

TABLE I Series of 10 first N^2 integer reflections for all crystalline systems. Series for bcc (body-centered cubic) and fcc (face-centered cubic) essentially apply to mono-elemental structures. sc = simple cubic lattice.

Crystalline system	Restrictions on h, k, l	Formula for N^2	10 first N^2 integer reflections									
Cubic: sc	None	$h^2 + k^2 + l^2$	1	2	3	4	5	6	8	9	10	11
Cubic: bcc	$h + k + 1$ even	$h^2 + k^2 + l^2$	2	4	6	8	10	12	14	16	18	20
Cubic: fcc	All even or odd	$h^2 + k^2 + l^2$	3	4	8	11	12	16	19	20	24	27
Tetragonal	$1 = 0$	$h^2 + k^2$	1	2	4	5	8	9	10	13	16	17
Hexagonal	$1 = 0$	$h^2 + hk + k^2$	1	3	4	7	9	12	13	16	19	21
Others	2 indices $= 0$	h^2 or k^2 or l^2	1	4	9	16	25	36	49	64	81	100

TABLE II Summary of microstructural analysis as a function of D and T for $Ga_{85}Mn_{15}$ and $Al_{73}Ni_{16}Ta_{11}$.

T(°C)	$D(10^{15}\,Ar^{++}\,cm^{-2})$: microstructure							
	$Ga_{85}Mn_{15}$				$Al_{73}Ni_{16}Ta_{11}$			
25	0	5: QC	22: QC	43: QC	0: Al	6: (Al)	13: (Al)	40: (Al)
80	0	5: QC	11: QC	27: QC	0: Al	9: (Al)	19: (Al)	53: (Al)
130	0	7: Cc	16: Cc	42: Cc	0: Al	17: (Al)	42: (Al)	70: (Al)
180	0	8: Cc	17: Cc	30: Cc	0: Al	5: QC	11: QC	27: QC
220	0: Cp	7: Cp	16: Cp	40: Cp	0: Al	5: QC	18: QC	60: QC
260	0: Cp	6: Cp	35: Cp	66: Cp	0: Al	12: QC	28: QC	46: QC
350	0: Cp	10: Cp	32: Cp	46: Cp	0: Al	4: QC	17: QC	29: QC

QC = quasicrystal; Al = Al(f c c); (Al) = Al partially amorphized (see text); Cp = crystalline diffraction pattern (points), Cc = crystalline diffraction pattern (circles). For $Ga_{85}Mn_{15}$ only, an amorphous phase was present in addition to those listed for all conditions given here.

We have not attempted to determine the exact crystalline structure, which would be readily recognized by observation of typical point patterns alone, as for $Ga_{85}Mn_{15}$ (see Table II). There is no quasicrystal in such a case, as it is highly unlikely that a quasiperiodic axis could not be observed (with a double-tilt stage) while its possible periodic axes (for quasicrystalline symmetries other than icosahedral) are observed. For $Ga_{85}Mn_{15}$, unidentified point patterns were often obtained, for any D or T value. This means that typical crystalline grain dimensions are of the order of a micrometre for this alloy. The amorphous phase was dominant for $D = 0$ from RT up to 180 °C. We did not observe Mn-α (b c c) for $D = 0$ at RT, as obtained in an analogous experiment by Knapp and Follstaedt during RT evaporation of Al–Mn multilayers [21].

Atomic mobility is increased at higher T, thus favouring larger grain dimensions. For a temperature high enough to give a point pattern with the smallest diaphragm size, a given phase can also be viewed as a circular pattern by using a larger size. This high-T circular pattern can then be used at lower temperatures to identify (as crystalline or quasicrystalline) identical patterns, which would otherwise be difficult to identify. For $Ga_{85}Mn_{15}$, this idea was applied at high T(220 °C < T < 350 °C) to identify crystalline circular patterns, noted Cc in Table II. From these observations, a good estimate on crystalline grain dimensions can be obtained from the diaphragm sizes (1, 2 and 5 μm). At high T, by changing diaphragm sizes a more or less complete circular pattern could be obtained from a point pattern, and grain dimensions were deduced to be typically a few micrometres (less than 5 μm) in this case. Otherwise, if grain dimensions were somewhat greater than 5 μm, this gross cellular pattern would not appear and if grain dimensions were somewhat smaller than 1 μm, no point pattern would be achieved by using the smallest diaphragm size. At low T, as very well defined circular patterns were always obtained with the smallest diaphragm size, grain dimensions were much smaller than 1 μm (by at least one order of magnitude), and could be determined in the same way by using much smaller diaphragm sizes, which were not available. For T > 130 °C, we noted an increase in concentration of crystalline phases with T or D. However, the amorphous phase was always present at any implantation conditions. The crystalline phases may not be unique, given the variety of observed point patterns. For $D' > 0$, the quasicrystalline phase is the dominant phase at RT and 130 °C, but has not been observed at higher temperatures. Given such a low transformation temperature, between 130 and 180 °C, it is likely that this phase is metastable.

For $Al_{73}Ni_{16}Ta_{11}$, the results were simpler and clearer as there were no observed points in patterns and the quasicrystalline phase was distributed over the entire surface of the specimen, with the result that no changes occurred in diffraction patterns when the electron beam spanned the surface. Given non-negligible variations in relative concentrations of the order of a few percent that exist between our various samples, the fact that the same results are obtained for various entries in Table II indicates a composition range for quasicrystal formation of similar magnitude. The observation of circular patterns means that grain dimensions are much smaller than one micrometre.

From Table II, using our evaporation rate, it can be seen that Al is crystallized under its unique stable form f c c by evaporation at RT, and is stable under heating only ($D = 0$) until at least 350 °C. We cannot exclude the possibility that the $Al_{73}Ni_{16}Ta_{11}$ quasicrystal could be produced by interdiffusion of elemental layers as a minimum temperature of 400 °C [22] was necessary for $Al_{80}Ru_{20}$, although a lower value has been observed for $Al_{86}Mn_{14}$ (270 °C) [22]. Furthermore, Al was partially amorphized below 180 °C, which was indicated by the presence of the first few reflection lines only. Although amorphous or crystalline phases other than Al (f c c) should be present, since Ta and Ni account for about 27% in atomic concentration and, in addition, a thin layer of alumina (spinel structure) must also be present at the surface of the specimens, these phases were not perceptible. In addition, there is the possibility of oxygen or nitrogen incorporation during electron-gun evaporation of the multilayered films, and during their subsequent treatment by ion bombardment. Several studies have shown, by using experimental conditions very similar to ours (e.g. a base pressure of 5×10^{-5} Torr during evaporation of multilayered samples [25]) that this possibility is negligible and does not affect the formation of well-known quasicrystalline alloys such as

$Al_{86}Mn_{14}$. Also, one work found that oxygen was essentially present on the surface of the specimens after irradiation, by forming a layer of about 5 nm in thickness [21]. Finally, the formation temperature (180 °C) is typical of that of other Al-based binary or ternary quasicrystals formed by ion-beam mixing or by a similar technique such as the implantation of Mn ions into Al (f c c) to form the $Al_{86}Mn_{14}$ quasicrystal [23].

3.2. Microstructural analysis for $Ga_{85}Mn_{15}$

The analysis was performed on a circular diffraction pattern, as shown in Fig. 1, and is summarized in Table III. Remarkably, the quasicrystal model accounts for all observed reflections without any omission, within the experimental uncertainty that, from the Al (f c c) diffraction data analysis (see below), has been determined to be $\pm$ 0.3 mm or about 1% in relative precision. Measurements were done manually with a micrometer and the uncertainty depends primarily on the precise localization of the centre of the diffraction ring. Such an agreement is unlikely to be just a coincidence and lends strong support to the presence of a quasicrystal. Even though this is not a point pattern, it can nevertheless be assigned to an icosahedral symmetry as the pattern has been indexed according to that symmetry. We cannot assign with equal or better precision values of Q_0^2 other than those indicated in Table III. The intensities and reflections are very different from those of the $Al_{86}Mn_{14}$ quasicrystal, which means that the Bancel *et al.* indexing [36] cannot be applied directly for our diffraction pattern. Clearly, this pattern is not from a cubic phase because no reasonable series of N^2 integer reflections has been found by multiplying $(R/R_1)^2$ ratios by $1 \leq N_{ref}^2 \leq 10$. If it is supposed that all reflections with two vanishing Miller indices were present, no crystalline phase would be suitable as the reflection $N^2 = 4$ is too far from the two nearest observed reflections: $(73.5/2R_1)^2 = 3.61$ and $(88.6/2R_1)^2 = 5.24$, where $2R_1 = 38.7$ mm. From powder diffraction files [40], we looked at all stable or metastable phases known to contain Ga or Mn alone, or both of these. All of these patterns were very different from ours, both in intensities and in interplanar spacings or ratios of *d*s. Neither did Villars and Calverts' compilation [41], nor stable [42] or metastable [43] phase diagrams

$Ga_{85}Mn_{15}$

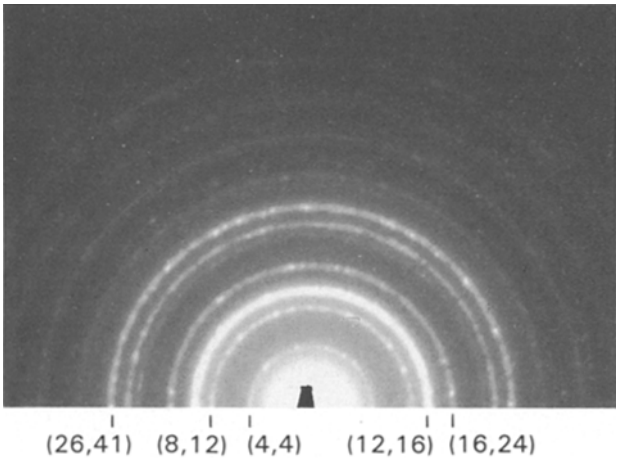

Figure 1 Quasicrystalline diffraction pattern for the $Ga_{85}Mn_{15}$ alloy obtained at $T = 80$ °C and $D = 11 \times 10^{15} Ar^{++}$ cm^{-2}. Indexation (N, M_0) is shown for several reflections. Complete indexation can be found in Table III.

TABLE III Analysis of the $Ga_{85}Mn_{15}$ quasicrystalline diffraction pattern (Fig. 1) observed below $T = 130$ °C, following the procedure established in Section 2.

I_{obs}	$2R$(mm)	$(R/R_1)^2$	N	M_0	Q_0^2	Q_0^2/Q_1^2	δ(%)	Q'	$2(R/R_2)^2$	$(hkl):N^2$	QC?
M	38.7	1	4	4	10.47	1	–	2.00	0.76	–	1
M	62.6	2.62	8	12	27.42	2.619	0.1	1.24	2	(110):2	–
S	73.5	3.61	12	16	37.89	3.619	0.3	2.35	2.77	–	3.61
M	88.6	5.24	16	24	54.83	5.237	0.1	1.75	4.01	(200):4	–
VW	96.0	6.15	18	29	64.92	6.201	1.3	0.45	4.71	–	6.15
W	108.4	7.85	24	36	82.25	7.856	0.1	2.14	6.00	(211):6	–
M	115.2	8.86	26	41	92.34	8.819	0.5	1.32	6.74	–	8.86
M	125.5	10.5	32	48	109.7	10.47	0.5	2.47	8.08	(220):8	–
VW	130.5	11.4	34	53	119.8	11.44	0.6	1.80	8.71	–	11.4
VW	140.8	13.2	38	61	136.7	13.06	1.4	0.89	10.0	(310):10	–
W	147.2	14.5	44	68	154.0	14.71	1.6	2.27	11.1	–	14.5
VW	153.7	15.8	46	73	164.1	15.68	1.1	1.52	12.0	(222):12	–
VW	167.6	18.8	56	88	198.4	18.95	1.0	2.05	14.4	(321):14	–
W	172.2	19.8	58	93	208.5	19.91	0.6	1.17	15.1	–	19.8
VW	177.6	21.0	62	97	219.0	20.91	0.7	2.32	16.1	(400):16	–
VW	189.8	24.1	70	113	252.8	24.15	0.4	0.65	18.5	(411):18	–
VW	192.2	24.9	72	116	259.7	24.80	0.5	0.90	18.9	–	24.9
W	194.5	25.3	74	117	263.3	25.15	0.4	2.10	19.3	–	25.3
VW	199.4	26.6	78	125	280.3	26.77	0.8	1.40	20.4	(420):20	–
VW	212.5	30.2	88	140	314.5	30.04	0.4	1.97	23.0	(332):22	–
W	219.0	32.0	94	149	335.1	32.01	0.0	2.24	24.5	(422):24	–
VW	231.1	35.7	104	160	371.8	35.51	0.4	2.32	27.2	(510):26	–
VW	263.5	46.4	150	240	488.3	46.64	0.6	1.14	35.7	(600):36	–

I_{obs} visually observed intensity. S = strong, M = medium, W = weak, VW = very weak. Some VW reflections are barely visible. $2R_1 = 38.7$ mm, $2R_2 = 62.6$ mm. $\delta(\%) = 100\{1 - (R/R_1)^2/(Q_0^2/Q_1^2)\}$.

provide other possible interpretations of the diffraction pattern. Therefore it may be concluded that no single crystalline phase can explain the present data.

There remains the possibility that at least two crystalline phases are present in the diffraction data. Although it is difficult to review all possibilities, nothing was found to match. However, as indicated in Table III by Miller indices and corresponding N^2, a part of the data is indexed on a bcc structure as is Mn-α [44], but for this latter structure some of the reflections observed are missing. This might be due to another form of Mn: these reflections may not belong to the quasicrystalline structure, which should be revealed by the other reflections, as indicated by values of $(R/R_1)^2$ in the last column of Table III under the "QC?" heading. For the reasons mentioned above, these remaining quasicrystalline reflections could not be indexed to any known or probable crystalline phases.

Finally, no correlation is observed from Table III between I_{obs} and Q'. This discrepancy should not be interpreted as a failure of the quasicrystalline model; rather, structure factor calculations using different atomic form factors and more refined decoration models that have not been investigated here should show a much better agreement. It is possible to estimate the value of d_0 from experimental conditions. From the $(N, M_0) = (32, 48)$ reflection we obtained $d_0 = 1.50$ nm, which is comparable to 1.747 nm obtained with $Al_{86}Mn_{14}$ [37]. This value represents a very large approximating cubic lattice, which can be estimated by considering rational approximants p_n/q_n of τ [45]. Replacing τ by p_n/q_n amounts to multiplying the interplanar spacing by $(q_n)^{1/2}$ in order to have all integer indices. To our experimental precision (1%) corresponds the approximant 8/5, that gives the minimum cubic interplanar spacing d_{min} compatible with the present data: $d_{min} = 5^{1/2}\ (15.0) = 3.34$ nm. Considering nearest-neighbour interatomic distances of 0.2 nm, this implies more than 5000 atoms per cubic cell.

3.3. Microstructural analysis for $Al_{73}Ni_{16}Ta_{11}$

Fig. 2 shows the Al(fcc) diffraction pattern whose

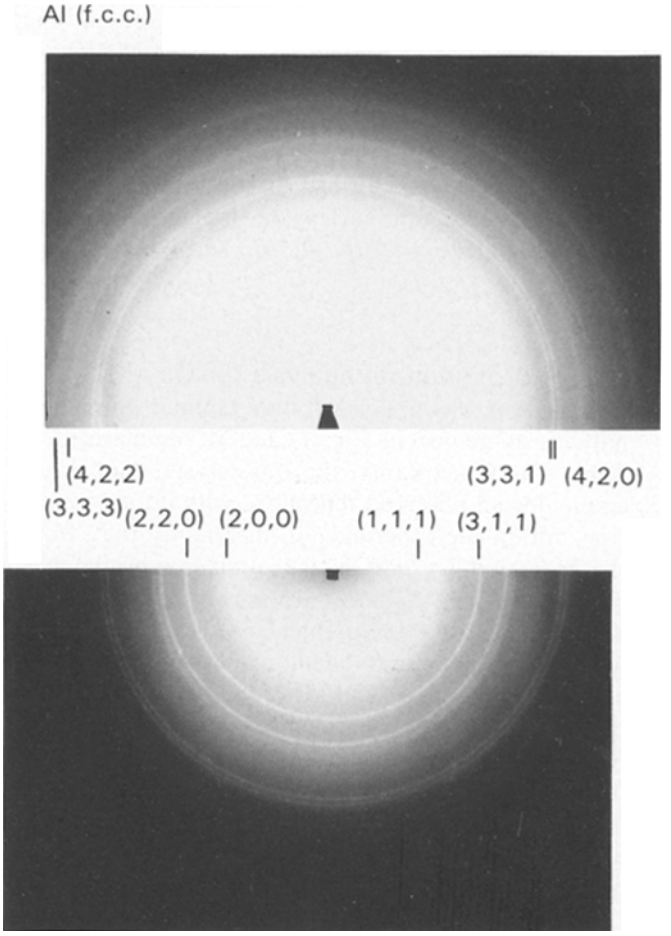

Figure 2 Diffraction pattern of Al(fcc) obtained at $T = 80\,^{\circ}C$ and $D = 0$. Because of the intense central spot (due to the undeflected electron beam), the pattern has been reproduced twice to show the maximum number of reflections, by using two different exposure times. Some of the reflections are indexed with Miller indices (h k l), which are included in Table IV. (a) High-index weakest reflections, (b) low-index strongest reflections.

analysis is summarized in Table IV. A good agreement is seen between observed and theoretical values of diameters.

A quasicrystalline phase has been obtained for $D > 0$, uniformly distributed from $T = 180$ to $T = 350\,^{\circ}C$. The minimum temperature of quasicrystalline formation for ion-beam mixing is therefore situated

TABLE IV Analysis of Al(fcc) diffraction pattern (Fig. 2) following the procedure established in Section 2.

I_{obs}	I_x	$2R$(mm)	$(R/R_1)^2$	$3(R/R_1)^2$	N^2	(hkl)	δ(%)
S	100	27.8	1	3	3	(1 1 1)	–
S	47	32.2	1.34	4.03	4	(2 0 0)	0.6
M	22	45.3	2.70	8.10	8	(2 2 0)	1.2
M	24	52.9	3.69	11.0	11	(3 1 1)	0.0
VW	7	55.3	4.02	12.1	12	(2 2 2)	0.4
VW	2	64.4	5.44	16.3	16	(4 0 0)	1.9
W	8	69.1	6.26	18.8	19	(3 3 1)	1.1
W	8	71.5	6.70	20.1	20	(4 2 0)	0.6
W	8	78.3	8.05	24.2	24	(4 2 2)	0.6
W	–	83.7	9.07	27.2	27	(3 3 3)	0.7
VW	–	91.4	10.8	32.4	32	(4 4 0)	1.3
VW	–	94.4	11.7	35.1	35	(5 3 1)	0.3
VW	–	96.3	12.0	36.0	36	(6 0 0)	0.0
VW	–	102.8	13.7	41.0	43	(5 3 3)	4.6

I_x = X-ray intensity [40]. $2R_1 = 27.8$ mm. $\delta(\%) = 100\,\{1 - (3(R/R_1)^2/N^2)\}$. Abbreviations as in Table III.

TABLE V Analysis of $Al_{73}Ni_{16}Ta_{11}$ quasicrystalline diffraction pattern (Fig. 3) observed at $180 \leq T(^{\circ}C) \leq 350$, following the procedure established in Section 2.

I_{obs}	$2R$(mm)	$(R/R_1)^2$	N	M_0	Q_0^2	Q_0^2/Q_1^2	δ(%)	Q'	$3(R/R_2)^2$	$(h\ k\ l)$, N^2; I_{obs}
W	48.9	1	4	4	10.47	1	–	2.00	1.15	–
M	79.1	2.62	8	12	27.42	2.619	0.1	1.24	3	(1 1 1):3; S
M	84.1	2.96	10	13	31.03	2.964	0.3	2.27	3.39	–
S	92.2	3.56	12	16	37.89	3.619	1.8	2.35	4.08	(2 0 0):4; S
VW	104.4	4.56	14	21	47.98	4.583	0.5	1.64	5.23	–
VW	112.0	5.25	16	24	54.83	5.237	0.2	1.75	6.01	–
VW	121.4	6.16	18	29	64.92	6.201	0.6	0.45	7.07	–
W	130.0	7.07	22	33	75.40	7.202	1.9	2.05	8.10	(2 2 0):8; M
VW	137.8	7.94	24	36	82.25	7.856	1.1	2.14	9.10	–
VW	153.2	9.82	30	45	102.81	9.819	0.0	2.39	11.3	(3 1 1):11; M
W	157.6	10.4	32	48	109.67	10.47	0.8	2.47	11.9	(2 2 2):12; VW
VW	183.5	14.1	42	65	147.17	14.06	0.1	2.19	16.1	(4 0 0):16; VW
VW	207.8	18.1	52	84	187.91	17.95	0.6	0.47	20.7	(4 2 0):20; W

See Table III for abbreviations and text for additional information. I_{obs} in the last column refers to observed Al(fcc) intensities.

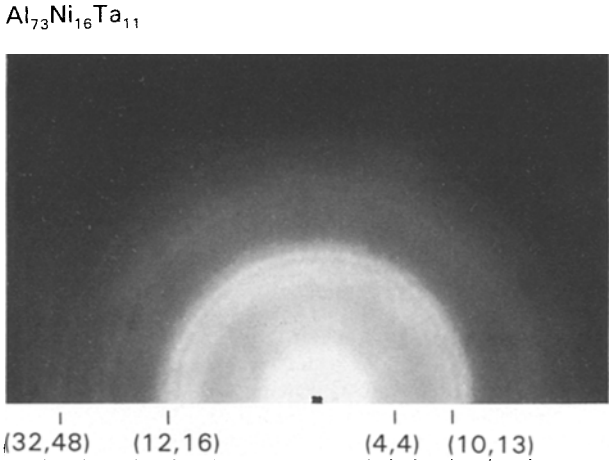

Figure 3 Quasicrystalline diffraction pattern for the $Al_{73}Ni_{16}Ta_{11}$ alloy obtained at $T = 260\,^{\circ}C$ and $D = 12 \times 10^{15} Ar^{++}\ cm^{-2}$. Indexation (N, M_0) is shown for several reflections. Complete indexation can be found in Table V.

between 130 and 180 °C, as can seen from Table II, which is comparable with other results obtained in the literature. It is possible that the quasicrystal $Al_{73}Ni_{16}Ta_{11}$ may be stable up to the melting point although this has not been checked. The diffraction pattern is shown in Fig. 3 and the corresponding analysis summarized in Table V. As in $Ga_{85}Mn_{15}$, the quasicrystalline model accounts for all observed reflections without any omission. Moreover, almost all of the first 15 quasicrystalline reflections are observed, which strengthens this identification. The intensities and reflections are very different compared to $Al_{85}Mn_{15}$ and $Ga_{85}Mn_{15}$. Also, the pattern in Fig. 3 for the latter cannot be from the $Al_{85}Ni_{15}$ quasicrystal as the strongest reflection is the same as for $Al_{85}Mn_{15}$, i.e. the $(N, M_0) = (18, 29)$ reflection [46].

The $Al_{85}W_{15}$ quasicrystal [8] (and in general quasicrystals of the form $Al_{85}TM_{15}$), show similar diffraction patterns [46] where TM is a 3d or 4d transition metal. We can therefore exclude the possibility that our quasicrystal is a binary one, Al–Ta. As before, one can assign a value to d_0. Using the $(N, M_0) = (8, 12)$ reflection, which coincides with the (1 1 1) reflection of Al(fcc), we find: $d_0 = aQ_0/3^{1/2} = 4.04(5.236)/3^{1/2} = 1.224$ nm where $a = 0.405$ nm is the Al(fcc) cubic side length. This value for d_0 is quite different from those of binary quasicrystals, which range from 1.677 to 1.817 nm for 3d TM [46], suggesting a very different microstructure from the binary ones. Using the 8/5 approximant, we obtain $d_{min} = 5^{1/2}12.24 = 2.74$ nm and more than 2600 atoms to the smallest crystalline cubic cell consistent with our data. As can be seen in the last column of Table V, some reflections have been reasonably indexed on Al(fcc), as indicated by Miller indices and N^2. However, the intensities do not match those we observed for Al(fcc), as indicated by I_{obs}. It is therefore concluded that it cannot be Al(fcc), although the quasicrystal microstructure might be closely related to it. Following the same analysis procedure as before, it was not possible to index the diffraction pattern to one or more crystalline phases for the same reasons, including extensive searches through [40, 41] as well as binary phase diagrams [47]. No ternary phase diagram on the Al–Ta–Ni system appears to be available. Finally, we conclude for this alloy the presence of a new quasicrystalline phase.

4. Conclusion

By ion-beam mixing, and by a simple microstructural analysis based on electron diffraction of two predictions ($Ga_{85}Mn_{15}$ and $Al_{73}Ni_{16}Ta_{11}$) made by means of quantum structural diagrams [3], experimental verification of two new quasicrystals has been obtained. The diffraction patterns of the quasicrystals obtained are very different from all those obtained from other quasicrystals, although comparable values were found for the quasicrystalline lattice constant d_0. Moreover, it is estimated that more than 5000 and 2600 atoms (for $Ga_{85}Mn_{15}$ and $Al_{73}Ni_{16}Ta_{11}$, respectively) for the smallest approximating cubic cells are consistent with the data and with experimental uncertainty. While these results strongly support our predictions, further experimental work would be warranted on the microstructural relations, (if any), between these two quasicrystals and others. However, it

is not certain that the actual compositions of the quasicrystals obtained are those indicated by the predictions. For example, the presence of an amorphous phase in the $Ga_{85}Mn_{15}$ samples at all irradiation conditions could conceivably affect the actual composition of the quasicrystalline phase.

As the list of known quasicrystals, which now comprises over 100 different metallurgical systems, grows continuously, all of these findings may suggest in the long term that the quasicrystalline state is not an exceptional state of solid matter after all. Whether this is true or not, there remains much progress to be made in comprehending the origin of quasicrystallinity, both from theoretical and experimental aspects. Nevertheless, our theoretical work [3] has shown that the chemical stability of quasicrystals can be accurately characterized (within a very small fraction of all possible metallurgical systems) by the proper use of a few general and highly significant atomic properties such as the electronegativity, valence and effective size. From this point of view, quasicrystals represent a third fundamental state of solid matter on an atomic scale, along with crystals and amorphous solids.

References

1. D. SHECHTMAN, I. BLECH, D. GRATIAS and J. W. CAHN, *Phys. Rev. Lett.* **53** (1984) 1951.
2. S. J. POON, A. J. DREHMAN and K. R. LAWLESS, *ibid.* **55** (1985) 2324.
3. J. TARTAS and E. J. KNYSTAUTAS, *J. Mater. Res.* **6** (1991) 1219.
4. J. A. ALONSO and N. H. MARCH, "Electrons in Metals and Alloys" (Academic Press, London, 1989).
5. K. M. RABE, A. R. KORTAN, J. C. PHILLIPS and P. VILLARS, *Phys. Rev. B* **43** (1991) 6280.
6. W. OHASHI and F. SPAEPEN, *Nature* **330** (1987) 555.
7. K. YU-ZHANG, PhD thesis, Université Paris VI, 1988.
8. P. A. BANCEL and P. A. HEINEY, *J. Phys. Colloq.* **47** (1986) C3-341.
9. J. F. ZIEGLER, J. P. BIERSACK and U. LITTMARK, "TRIM-89: Transport of ions in matter," Version 5.3 (IBM Research, Yorktown Heights, New York, 1989).
10. U. LITTMARK and J. F. ZIEGLER, "Handbook of range distributions for energetic ions in all elements" (Pergamon, New York, 1980).
11. A. F. BURENKOV, F. F. KOMAROV, M. A. KUMAKHOV and M. M. TEMKIN, "Tables of ion implantation spatial distributions" (Gordon & Breach, New York, 1986).
12. D. A. LILIENFELD, in "Fundamentals of beam-solid interactions and transient thermal processing," edited by M. J. Aziz, L. E. Rehn and B. Stritzker (Materials Research Society Symposium Proceedings 100, Pittsburgh, 1989) p. 45.
13. C. H. SHANG, J. LI, H. D. LI and B. X. LIU, *J. Phys. F* **18** (1988) L169.
14. D. M. FOLLSTAEDT and J. A. KNAPP, *Mater. Sci. Engng.* **99** (1988) 367.
15. J. A. KNAPP and D. M. FOLLSTAEDT, in "Fundamentals of beam-solid interactions and transient thermal processing," edited by M. J. Aziz, L. E. Rehn and B. Stritzen (Materials Research Society Symposium Proceedings 100, Pittsburgh, Pennsylvania, 1989) p. 45.
16. K. HOHMUTH, V. HEERA and B. RAUSCHENBACH, *Nucl. Instr. Meth. Phys. Res.* **B39** (1989) 136.
17. B. RAUSCHENBACH and V. HEERA, *J. Mater. Sci. Lett.* **6** (1987) 401.
18. L. M. GRATTON, A. MIOTELLO, C. TOSELLO, D. C. KOTHARI, G. PRINCIPI and A. TOMASI, *Nucl. Instr. Meth. Phys. Res.* **B59/60** (1991) 541.
19. D. M. FOLLSTAEDT and J. A. KNAPP, *Mater. Sci. Engng.* **90** (1987) 1.
20. D. M. FOLLSTAEDT and J. A. KNAPP, *J. Appl. Phys.* **59** (1987) 1756.
21. J. A. KNAPP and D. M. FOLLSTAEDT, *Phys. Rev. Lett.* **55** (1987) 1591.
22. D. A. LILIENFELD, M. NASTASI, H. H. JOHNSON, D. G. AST and J. W. MAYER, *ibid.* **55** (1987) 1587.
23. J. D. BUDAI and M. J. AZIZ, *Phys. Rev. B* **33** (1987) 2876.
24. L. J. HUANG, B. X. LIU and H. D. LI, *ibid.* **41** (1990) 9523.
25. L. J. HUANG and B. X. LIU, *Nucl. Instr. Meth. Phys. Res.* **B18** (1987) 256.
26. N. KARPE, L. U. AAEN ANDERSEN, K. DYRBYE, J. BOTTIGER and K. V. RAO, *Phys. Rev. B* **39** (1989) 9874.
27. D. A. LILIENFELD, L. S. HUNG and J. W. MAYER, *MRS Bull.* **12** (1987) 31.
28. D. A. LILIENFELD, J. W. MAYER, M. NASTASI, E. RIMINI and B. M. ULLRICH, *Nuovo Cimento D* **7** (1986) 134.
29. D. A. LILIENFELD, M. NASTASI, H. H. JOHNSON, D. G. AST and J. W. MAYER, *J. Mater. Res.* **2** (1986) 237.
30. J. A. EADES, in "Encyclopedia of material sciences and engineering," Vol. 6, edited by M. B. Bever (Pergamon, Oxford and MIT, Cambridge, 1988) p. 535.
31. P. M. OSSI, *Mater. Sci. Engng.* **A115** (1989) 107.
32. P. J. STEINHARDT, *Mater. Sci. Forum* **22–24** (1987) 23.
33. M. AUDIER and P. GUYOT, in "Extended icosahedral structures (Aperiodicity and order)," Vol. 3, edited by M. V. Jaric and D. Gratias (Academic, Boston, 1988) ch. 1.
34. P. W. STEPHENS, in "Extended icosahedral structures (Aperiodicity and order) " Vol. 3, edited by M. V. Jaric and D. Gratias (Academic, Boston, 1988) ch. 3.
35. S. MATTESON et M. A. NICOLET, in "Mestastable materials formation by ion implantation," edited by S. T. Picraux and W. J. Choyke, (Materials Research Society Symposium Proceedings 7, Amsterdam, 1982) p. 3.
36. P. A. BANCEL, P. A. HEINEY, P. W. STEPHENS, A. I. GOLDMAN and P. M. HORN, *Phys. Rev. Lett.* **54** (1985) 2422.
37. J. W. CAHN, D. SHECHTMAN and D. GRATIAS, *J. Mater. Res.* **1** (1986) 13.
38. V. ELSER, *Phys. Rev. B* **32** (1985) 4892.
39. C. KITTEL, "Introduction to solid state physics," 5th edn Wiley, New York, 1976).
40. Avon, "Powder diffraction files, alphabetical Index, inorganic phases, 1988," (International Centre For Diffraction Data, Swarthmore, Pennsylvania, 1988).
41. P. VILLARS and L. D. CALVERT, "Pearson's handbook of crystallographic data for intermetallic phases," (American Society of Metals, Metals Park, Ohio, 1985).
42. S. S. LU, J. K. LIANG and T. J. SHI, *Acta Phys. Sinica* **29** (1980) 469.
43. V. N. GUDZENKO and A. F. POLESYA, *Russ. Metall.* **5** (1976) 153.
44. J. EMSLEY, "The Elements," (Clarendon, Oxford, 1987).
45. D. GRATIAS, R. MOSSERI, J. PROST, J. TONER and M. DUNEAU, "Du cristal à l'amorphe (From crystalline to amorphous)," (Les éditions de physique, Les Ulis Cedex, France, 1987).
46. R. A. DUNLAP and K. DINI, *J. Phys. F* **16** (1986) 11.
47. W. G. MOFFAT, "The handbook of binary phase diagrams," (Genium Publishing Corp., New York, 1984).

Received 28 January
and accepted 6 October 1993